PHILOSOPHICAL TRANSACTIONS OF THE ROYAL SOCIETY B BIOLOGICAL SCIENCES

Efficiency and Evolution of Water Transport Systems in Higher Plants: A Modelling Approach. I. The Earliest Land Plants

A. Roth, V. Mosbrugger and H. J. Neugebauer

Phil. Trans. R. Soc. Lond. B 1994 **345**, 137-152
doi: 10.1098/rstb.1994.0093

Efficiency and evolution of water transport systems in higher plants: a modelling approach. I. The earliest land plants

A. ROTH[1], V. MOSBRUGGER[1] AND H. J. NEUGEBAUER[2]

[1]*Institut und Museum für Geologie und Paläontologie der Universität Tübingen, Sigwartstr. 10, D-72076, Tübingen, Germany*
[2]*Institut für Geodynamik, Universität Bonn, Nußallee 8, D-53115, Bonn, Germany*

SUMMARY

The evolution of the stele was studied under the functional aspect of water transport problems by using a numerical approach. The underlying mathematical model describes the behaviour of a fluid-filled porous medium and is based on the coupling of Hooke's law and Darcy's law including a dynamic permeability approach which leads to a self-organization of the considered structure according to the resulting fluid-pressure field. Calculations dealing with two problems were performed. The essential demand of a water conducting system for a plant was demonstrated quantitatively. As soon as the plant shows an upright habit, the need for efficient water transport occurring through a highly porous apoplastic pathway becomes evident. In a second approach, the evolution of the protostele was simulated using the concept of dynamic permeability. The simulations of structures with self-regulating hydraulic conductivity yielded two strategies according to the pressure–permeability relationship. Increasing hydraulic conductivity with increasing negative fluid pressure results in peripheral layers of the conducting tissues, whereas the inverse pressure–permeability relationship yields a central position of the conducting tissues. The latter arrangement corresponds to the protostelar construction of early vascular plants.

1. INTRODUCTION

The colonization of land by higher plants in the Upper Silurian or even earlier (Edwards & Fanning 1985; Gray 1985) was one of the crucial steps in the evolution of the planet earth and its ecosystems. For the plants this step from the water onto the land opened a new and large field of ecological licences but confronted them with a totally different environment and correspondingly with a series of new problems. In a water environment there are no serious obstacles to reproduction and fertilization and male and female gametes can be released directly into the water. In a terrestrial environment, however, sexual reproduction is more difficult to accomplish and hence land plants developed numerous adaptations of their life cycle (e.g. seeds) to cope with this problem (cf. Bower 1908; Stebbins & Hill 1980). Gravity is another serious problem in terrestrial environments. Its relevance for the evolution of higher land plants has been analysed in various papers and it was demonstrated that evolutionary changes in growth habits of land plants were largely constrained by gravity (e.g. Niklas 1984; Speck & Vogellehner 1988; Mosbrugger 1990).

A third problem of land plants relates to the water budget. Land plants are surrounded by air which generally has a negative water potential and hence acts as a desiccating medium. Some smaller land plants such as algae, lichens or mosses can resist desiccation or are restricted to habitats with a high atmospheric moisture content and can take up water directly over their surface. In contrast, higher land plants (tracheophytes) have developed a complex set of adaptations to colonize drier habitats and to maintain a balanced water budget (Raven 1984). To compensate for the water loss due to transpiration these homoiohydric plants take up water from the soil and transport it to the sites of transpiration. This transport occurs in a vascular bundle with dead elongated cells (tracheids, vessels) and the transport energy is provided by the water potential gradient between the air and the soil. To minimize and regulate the transpiration rate a cuticle and stomata are developed.

Although we can understand the basic adaptations of the various groups of land plants to solve this problem of water loss and transpiration many questions remain. For instance, the detailed mechanisms of water uptake and water transport in the various tissue types (e.g. xylem, parenchyma) are still unclear (Molz & Ferrier 1982; Boyer 1985; Westgate & Steudle 1985; Canny 1989). In addition, our understanding of the evolution of the water transport system is relatively poor: we know that in plant axes as well as in leaves numerous different water transport systems evolved and sometimes we can even trace the evolutionary pathways (e.g. Zimmermann 1952) but we do not really understand the reasons for the observed evolution. In this and a series of other papers we will approach some of the questions related to the water transport in land plants. In particular we will

Phil. Trans. R. Soc. Lond. B (1994) **345**, 137–152
Printed in Great Britain

analyse the efficiency of various water transport systems in land plants and demonstrate that the necessity for an efficient water transport constrained the evolution of land plants in a similar way as did the problems of gravity and reproduction/fertilization. In this first study we will concentrate on the evolution of a stele in the earliest tracheophytes.

2. THE PROBLEM: EVOLUTION OF THE PROTOSTELE

The existence of a stele is the diagnostic character of tracheophytes. The oldest plant remains which show a vascular bundle with tracheids are from the Lower Devonian and belong to *Cooksonia pertonii* (Edwards *et al.* 1992) but possibly vascular bundles existed already in similar plant axes ('telomes') which occur in the Upper Silurian and which are also referred to *Cooksonia*. *Cooksonia pertonii* as well as some other early land plants (e.g. *Rhynia*) have their tracheids arranged in a central strand or protostele which is considered to be the most simple organization of a stele. A similar central strand consisting of hydroids can be found in some mosses (Proctor 1982).

According to Zimmermann (1959), the protostele can be derived from central strengthening structures of the land plants' algal ancestors. Zimmermann assumed that the water living predecessors of the tracheophytes had a central strengthening tissue which stabilized them mechanically against the forces occurring in the surf zone and indeed, such a tissue exists in various modern algae living in environments where considerable drag forces occur (Koehl & Wainwright 1977). He pointed out that the protostele of the earliest tracheophytes has to be considered as a relict of the mechanical system of algal ancestors (Zimmermann 1959). It is unlikely, however, that such large algae represent the ancestors of tracheophytes (Graham 1993). According to another view the architecture of the protostele is more related to photosynthesis. In a leafless plant axis or telome, as it exists in the most primitive tracheophytes, a central strand allows for a peripheral and exponated position of the photosynthesizing tissues (Carlquist 1975). This hypothesis, however, cannot explain why the earliest tracheophytes have a protostele and not a siphonostele or actinostele which are all central strands. In fact, Speck & Vogellehner (1988) have shown that protostele, siphonostele and actinostele do not differ significantly with respect to their mechanical properties.

As a whole, up till now there is no theory or concept which considers the stelar evolution in relation to water transport. In this paper we try to understand and explain the evolution of the protostele by analysing the water budget and water transport problems of the earliest land plants. Two different questions are considered and analysed with a computer modelling approach. First, we investigate whether land plants do indeed need a water conducting system and whether there is a maximum height up to which a plant is able to live in a desiccating terrestrial environment without a water conducting system. As a second problem the evolution of the protostele is simulated with a self-regulating system, which forms its internal hydraulic architecture according to defined hydrodynamic parameters. These problems are treated numerically using a mathematical model, which was originally designed to simulate fluid flow and mechanical reactions during porous rock compaction (Grün *et al.* 1989).

3. THE MODELLING APPROACH: NUMERICAL METHOD AND DEFINITION OF THE MODEL STRUCTURES

The model used for the following analyses considers a system, which is composed of two phases, porous material and fluid. The model system is based on the coupling of Hooke's law (mechanical deformation is reversible and proportional to mechanical stress) and Darcy's law (fluid flow is proportional to the fluid pressure gradient). The two phases are coupled and therefore react simultaneously to external forces and fluid flows. A mechanical load acting on one side, for example, will cause a fluid flow out of the region of deformation. In this way, mechanical behaviour and hydrodynamics of a given structure are connected. The mathematical model system itself is briefly discussed in the Appendix.

A coupled system of differential equations (for details see Appendix) is solved with a Finite Element (FE) approach. By using this method the structure (i.e. plant axis), which is to be analysed, is split into elements with defined geometrical properties. The elements are defined by a set of nodes or discrete points (the term 'node' is used here in a mathematical sense as coordinate point, whereas the botanical term 'node' denotes the point of leaf insertion on the plant stem; the term 'node' is always used in this paper as a synonym for 'discrete point'). The integration of the differential equations is performed numerically over the elements. As a result, the entire domain is represented by the behaviour of its subareas. For a detailed discussion of the Finite Element method see, for example, Zienkiewicz & Taylor (1989). The specific problem considered here and its solution is described in detail by Wallner (1990). The corresponding computer program NAPE (Wallner 1990) enables the user to perform calculations on arbitrary axisymmetric grids. An important feature of the algorithm is the possibility of defining very complex boundary conditions in order to obtain a realistic model structure. The unknown variables are: (i) displacement of the nodes in two directions, u_x and u_y; and (ii) the fluid pressure p at the nodes. The fluid pressure p is calculated as difference to the initial value of p ($= 0$) thus representing the excess fluid pressure. In the following, p will be denoted simply as fluid pressure or hydrostatic pressure, but p is always the difference from the initial value. In addition, it should be mentioned that p is not identical with the water potential Ψ which describes the water status of a plant tissue. Several quantities, including the hydrostatic pressure, contribute to Ψ (see, for example, Slatyer 1967).

As the problems analysed are time dependent, a discretization of time is necessary. The calculations are performed in time steps by numerical integration until the steady state condition (see below) is attained.

PHILOSOPHICAL TRANSACTIONS OF THE ROYAL SOCIETY B BIOLOGICAL SCIENCES

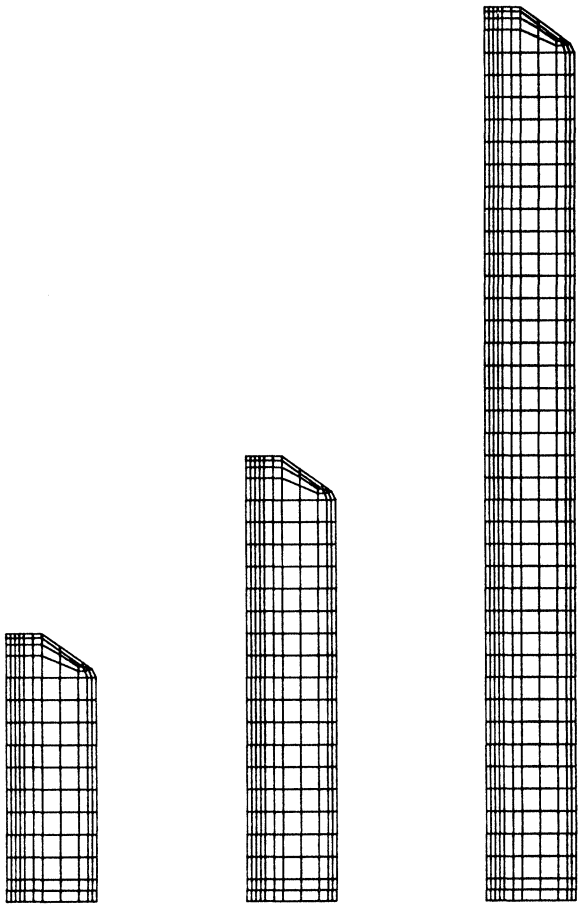

Figure 1. The grids representing the different axes which were used for the homogeneous model. The proportions of radius to length are: (*a*) (1:3); (*b*) (1:5); (*c*) (1:10).

By each computation step u_x, u_y and p are calculated for every single node point. Thus, solutions are given for all nodes and for all time steps t_n.

This basic model has been adapted for the analysis of the water transport efficiency in various plant axes or telomes with and without a vascular bundle.

(*a*) *The homogeneous model*

To analyse whether simple land plants could survive without a water transport system, water transport in simple (leafless) telome structures consisting entirely of parenchyma was modelled. For this purpose axisymmetric structures with homogeneous material properties and constant hydraulic conductivity were used. Different halfspaces, illustrated in figure 1 and summarized in table 1, were considered in order to get quantitative information about limitations of a purely parenchymatous water transport. Effects of gravity were neglected in this case. Note that the grids define axisymmetric halfspaces with the axis of rotation at the left.

In addition, appropriate boundary conditions had to be defined (for a mathematical description of the boundary conditions, see Bear 1979). First, the structures were fixed in space. This was achieved by choosing the Dirichlet boundary conditions at the bottom (X-axis) and along the axis of rotation (Y-axis). Thus, the nodes at the bottom are allowed to move parallel to the horizontal direction while the nodes on the rotational axis may perform displacements parallel to the vertical direction only. In addition, a free water inflow from the bottom into the structure was also modelled by the appropriate Dirichlet boundary conditions: for all nodes at the bottom the fluid pressure p was defined to be $p = 0 =$ constant. Thus, the bottom served as a free boundary with respect to the fluid pressure. In this way, water supply by absorbing underground organs was substituted by a fluid reservoir below the bottom of the axisymmetric structures. This simplification seemed to be reasonable as the fluid uptake into the plant should not be a limiting factor in our models and because a detailed modelling of water uptake and flow into the shoot was not intended. The transpiration driving water from the roots to the surface was simulated by a Cauchy boundary condition of a constant water outflow at the surface of the structure. The rate of transpiration was estimated from values

Table 1. *The set of different halfspaces which were used for the homogeneous model*
(Each structure corresponds with a concrete calculation.)

structure	proportion radius to height	radius mm	height mm	hydraulic conductivity ($mm^2\ s^{-1}\ kPa^{-1}$)	transpiration rate ($mm^3\ mm^{-2}\ s^{-1}$)
A1	1:3	0.25	0.75	10^{-6}	10^{-5}
A2	1:3	0.5	1.5	10^{-6}	10^{-5}
A3	1:3	1.0	3.0	10^{-6}	10^{-5}
A4	1:3	2.0	6.0	10^{-6}	10^{-5}
B1	1:5	0.25	1.25	10^{-6}	10^{-5}
B2	1:5	0.5	2.5	10^{-6}	10^{-5}
B3	1:5	1.0	5.0	10^{-6}	10^{-5}
B4	1:5	2.0	10.0	10^{-6}	10^{-5}
C1	1:10	0.25	2.5	10^{-6}	10^{-5}
C2	1:10	0.5	5.0	10^{-6}	10^{-5}
C3	1:10	1.0	10.0	10^{-6}	10^{-5}
C3b	1:10	1.0	10.0	10^{-6}	10^{-7}
C3c	1:10	1.0	10.0	10^{-7}	10^{-5}
C3d	1:10	1.0	10.0	10^{-7}	10^{-7}

PHILOSOPHICAL TRANSACTIONS OF THE ROYAL SOCIETY B BIOLOGICAL SCIENCES

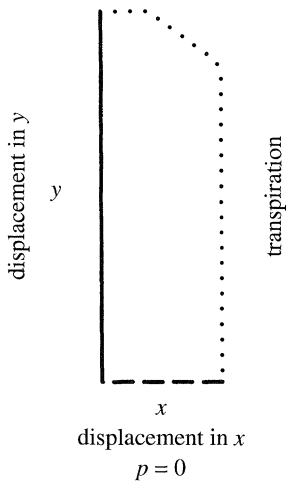

Figure 2. Boundary conditions of the model axes. The nodes at the axis of rotation (left axis) are allowed to move vertically, whereas the nodes at the bottom (= dashed line) may perform horizontal displacements. The fluid outflow (= transpiration) occurs over the surface which is represented by a dotted line.

found in higher plants today (Altman & Dittmer 1973). The process of evaporation itself was not included in the model simulations. The boundary conditions are summarized in figure 2.

The mathematical model used here is based on the assumption that the entire structure is linear elastic and mechanically isotropic. In most cases, this is not valid for biological materials (Vincent 1990). In addition, the material parameters of biological tissues are influenced by water content and number of cells (Falk *et al.* 1985; Niklas 1988). Interactions of water content and mechanical behaviour are complex phenomena (Schulte 1992). However, isotropic and linear elastic behaviour as well as constant material parameters were supposed to represent acceptable approximations in this case, because no additional mechanical loads with corresponding effects on the material matrix were used (the term material matrix will be used as synonym for the solid phase). Even a highly complex mechanical model, which could describe the mechanical behaviour of a certain tissue exactly, is expected to have little influence on the results with respect to the water transport dynamics.

If available, parameters for parenchymatous tissues were used in the homogeneous model. For a material under mechanical load, the modulus of elasticity (E-modulus or Young's modulus) describes the ratio of the applied stress and the resulting strain. For potato parenchyma, Niklas (1988) found this value to be between 5×10^3–1.9×10^4 kPa. For the apex of *Pisum sativum* seedlings, an E-modulus of about 4×10^4 kPa was measured (Burström *et al.* 1970). The value used in this study was 5×10^4 kPa. The Poisson-ratio describes the contraction of a material at a given strain in the case of mechanical loading. Because of an often anisotropic behaviour of biological material, an estimation of this value is difficult. For apple flesh, Chappell & Hamann (1968) measured values between 0.21–0.34. The compressibility is defined as reciprocal value of the modulus of compression. The latter describes the change of a structure's volume in the case of an overall loading. The compressibility of grain is related to the components building up the material matrix, not to the matrix itself. It is assumed for parenchyma, that the essential component is the water which shows a compressibility of 5×10^{-7} kPa^{-1}. However, as it is not the only component, this value was rounded up to 1×10^{-6} kPa^{-1}.

In general, apoplastic and symplastic pathways can be used in parenchymatous water transport (Molz 1976; Molz & Ferrier 1982). It is likely, that both are co-existing in many cases (Molz & Ferrier 1982; Boyer 1985; Canny 1989). Owing to the complex nature of water transport in parenchyma, it is difficult to give an exact value for the hydraulic conductivity of parenchyma. Raven (1977, 1984) estimated the upper limit to be 1×10^{-6} mm^2 s^{-1} kPa^{-1}. This value was varied for some of our modelling experiments. In these cases, the variations will be given explicitly for the corresponding model structures. The parameter of porosity, which is between 0 and 1, gives not the total void space, but the portion of the fluid which can move freely inside the material matrix (see, for example, Bear 1972; deMarsily 1986). This quantity is defined as: porosity = (free volume of fluid) × (total volume)$^{-1}$. In all living cells water is an essential constituent. If it is lost totally, the cell will loose its structure and properties. Therefore, a porosity of 0.3 is assumed for parenchyma, that is, a fraction of 30% of the water of the tissue can flow freely. Additionally, the model assumes the structure to be saturated with water. This means, in general, that a discontinuous fluid phase is not considered.

In our model the fluid flow inside the model structures considered are controlled by the mechanical properties, the hydraulic conductivities and the gradient of the fluid pressure. Thus, the plant tissue is represented macroscopically by its mechanical and hydraulic parameters and not by microscopic processes on the cellular level. Basically, parenchyma is composed of two porous continua. The cell walls can be described as a porous matrix (Nobel 1983), whereas the behaviour of the symplasm is determined by osmotic processes due to the cell membranes. Osmotic potential and turgor pressure define the 'water status' of a living cell. In the computer model used here, microscopic interactions are summarized to yield a macroscopic system, in which the parenchyma is represented by a homogeneous structure with defined permeability. The calculations yield the differences of fluid pressure, which are necessary for a given structure with the hydraulic conductivity of parenchyma to establish a water transport from the bottom (substrate) to the transpiring surfaces. Living tissue would generate the required gradient by the water potential. The material parameters used in the calculations are summarized in table 2.

(*b*) *Homogeneous model with dynamic permeability*

With a second model group the evolution of the protostele was analysed. Here, the same considerations regarding the parameters and boundary condi-

PHILOSOPHICAL TRANSACTIONS OF THE ROYAL SOCIETY B BIOLOGICAL SCIENCES

Table 2. *The material parameters applied for the homogeneous model structures*

(Hydraulic conductivity and transpiration rate were varied. These two values are given in table 1 together with the corresponding model structures.)

parameter	data	references
E-modulus	5×10^4 kPa	Burström *et al.* (1970), Niklas (1988)
Poisson-ratio	0.25	Chappell & Hamann (1968)
compressibility of grain (material)	1×10^{-6} kPa^{-1}	estimated
compressibility (fluid)	5×10^{-7} kPa^{-1}	Weast & Astle (1983)
porosity	0.3	estimated

tions were valid but the hydraulic conductivity was defined to be a function of the effective pressure (see equation (10) in the Appendix). Effective pressure means the difference between fluid pressure and mechanical pressure acting in the material matrix itself. In the case of our two model structures (A and B, see below) the effective pressure depended only on the fluid pressure. The hydraulic conductivity was therefore a function of the fluid pressure p. As a result, the model structures were able to adjust the hydraulic conductivity locally according to changes in fluid pressure. However, the hydraulic conductivity also influenced the fluid pressure in a feedback, because, at a given water outflow, the hydraulic conductivity determines the fluid pressure, which itself influences the hydraulic conductivity. Thus, a self-regulating system results in which the pattern of hydraulic conductivities was created by the feed-back of fluid pressure and permeability. This (purely theoretical) dynamical approach should reveal whether the evolutionary development of water-conducting tissues may be understood in terms of a self-regulating system in which apoplasmic permeability increases according to local pressure–flow relationships. The evolution of water-conducting tissues is thus modelled macroscopically as a process of self-organization controlled by defined physical parameters.

To study the patterns resulting from various relationships between hydraulic conductivity and effective pressure, two functions with antagonistic dependencies of permeability on pressure were chosen (see figure 3). The results will be compared with real architectures of conducting tissues afterwards.

Model A: Increase of hydraulic conductivity with increasing negative fluid pressure This means, that hydraulic conductivity increases with decreasing fluid pressure.

Model B: Decrease of hydraulic conductivity with increasing negative fluid pressure. This means, that

Table 3. *The values of* T_{stat} *which were found for the different halfspaces in the homogeneous model*

structure	time required to reach the steady state condition/s
A1[a]	30
A2[a]	110
A3[a]	600
A4[a]	2.000
B1[a]	100
B2	440
B3	1.800
B4	7.000
C1[a]	450
C2[a]	1.800
C3[a]	7.100
C3b	7.100
C3c	71.000
C3d	71.000

[a] Values used in figure 4.

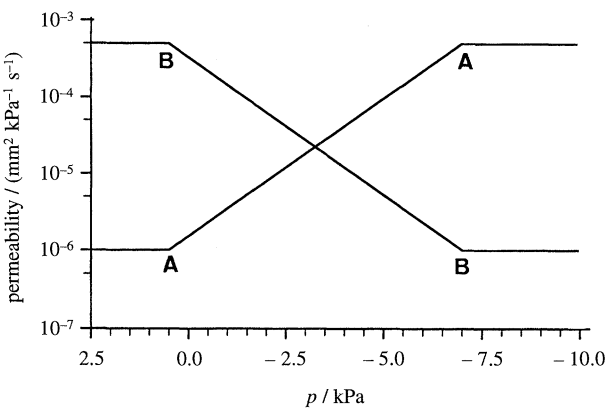

Figure 3. Two functions of defined dependence of hydraulic conductivity on fluid pressure. A, Increase of hydraulic conductivity with increasing negative fluid pressure. B, Decrease of hydraulic conductivity with increasing negative fluid pressure. The two functions were applied in the homogeneous model with dynamic permeability.

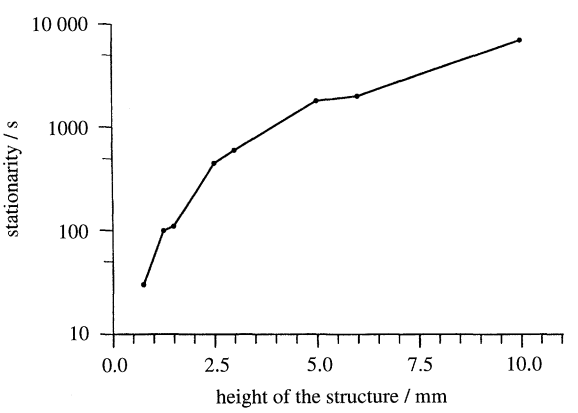

Figure 4. Plot of the values of T_{stat} (= time span required to reach the steady-state condition) against the height of the structures A1–C3 (see table 1) in a semilogarithmic representation.

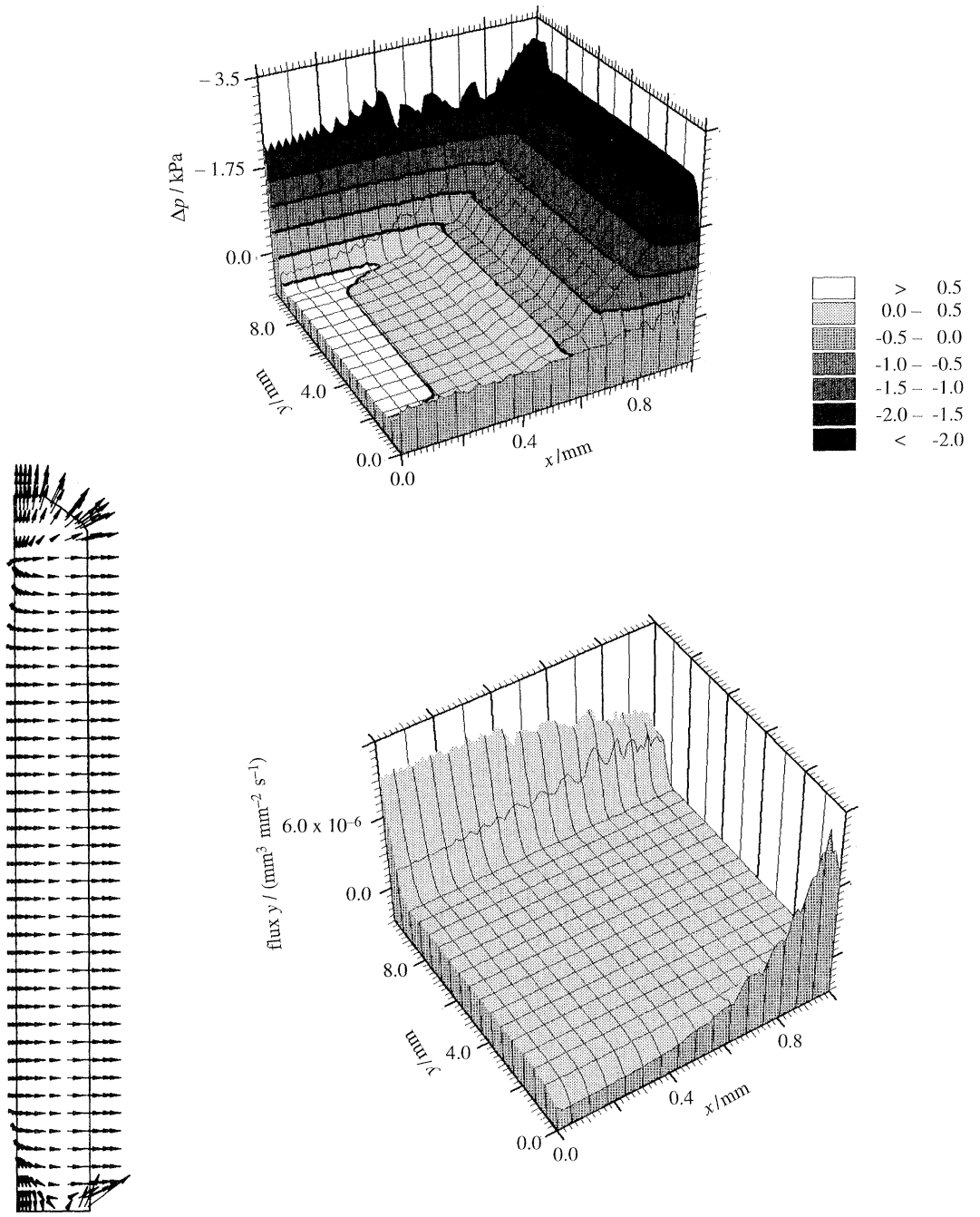

Figures 5–9. Structure C3 (radius = 1 mm, height = 10 mm, transpiration rate = 1×10^{-5} mm^3 mm^{-2} s^{-1}, hydraulic conductivity = 1×10^{-6} mm^2 s^{-1} kPa^{-1}); results obtained at discrete time values (s). The contour lines are equidistant starting with the least negative pressure values. Figure 5, $t_1 = 1$; figure 6, $t_2 = 10$; figure 7, $t_3 = 100$; figure 8, $t_4 = 1000$; and figure 9, $t_5 = 7100 = T_{stat}$. Represented are fluid velocities as vectors (lower left), pressure field as contours plotted against spatial coordinates (above) and the longitudinal component of the flow, v_y, against spatial coordinates (lower right).

the hydraulic conductivity decreases with decreasing fluid pressure.

The grid used for this model group is represented in figure 1*b*. Boundary conditions and all material parameters, with the exception of hydraulic conductivity and transpiration rate were the same as in the homogeneous model with constant hydraulic conductivity. A transpiration rate of 5×10^{-4} mm^3 mm^{-2} s^{-1} was chosen to yield a temporally fast reaction of the structure.

5. RESULTS

(*a*) *Homogeneous model with constant hydraulic conductivity*

First, model structures with varying dimensions but with identical material parameters were considered (structures A1–C3, see table 1). The structures differ with respect to the time span of the non-steady state. This is shown in table 3 and in figure 4. In this graph

PHILOSOPHICAL TRANSACTIONS OF THE ROYAL SOCIETY B BIOLOGICAL SCIENCES

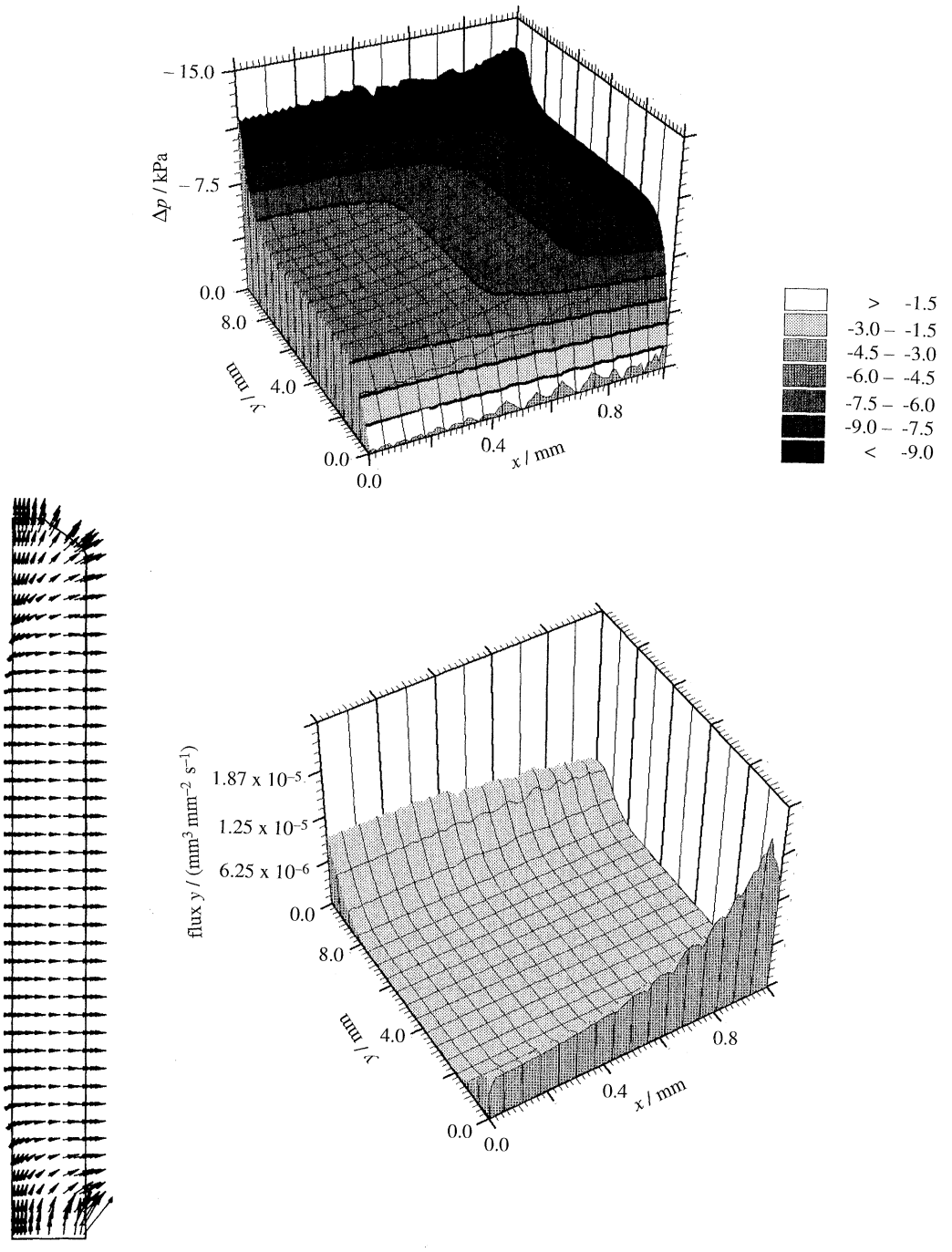

Figure 6. For description see figure 5.

the time span required by the different structures to reach the steady state condition (T_{stat}) is plotted against the height of the axis. Obviously, T_{stat} depends on the length of the path which defines the maximum distance between the sites of in- and outflow: the shorter the structure the faster stationarity is reached at a given hydraulic conductivity.

The development of fluid velocities and fluid pressure p are visualized in several graphs. For structure C3 (radius = 1 mm, length = 10 mm) the temporal development of these parameters is illustrated by showing the results at different time steps in figures 5–9 (figure 5, $t_1 = 1$ s; figure 6, $t_2 = 10$ s; figure 7, $t_3 = 100$ s; figure 8, $t_4 = 1000$ s; and figure 9, $t_5 = T_{stat} = 7100$ s). The results are presented as fluid velocities, fluid pressure field, and longitudinal component of the fluid velocity, v_y. Fluid velocities are summarized as vectors. Their length refers to the highest velocity which is represented by the maximum vector length. Fluid pressure p and v_y are plotted against spatial coordinates in a three-dimensional graph and represented as contour plots.

The graphs for each time step illustrate that a vertical water transport is slowly established. At t_1, only lateral fluxes exist. This is due to the pressure field which produces a gradient parallel to the X-axis. The corresponding contours are arranged mainly parallel to the longitudinal axis. Thus, the values of

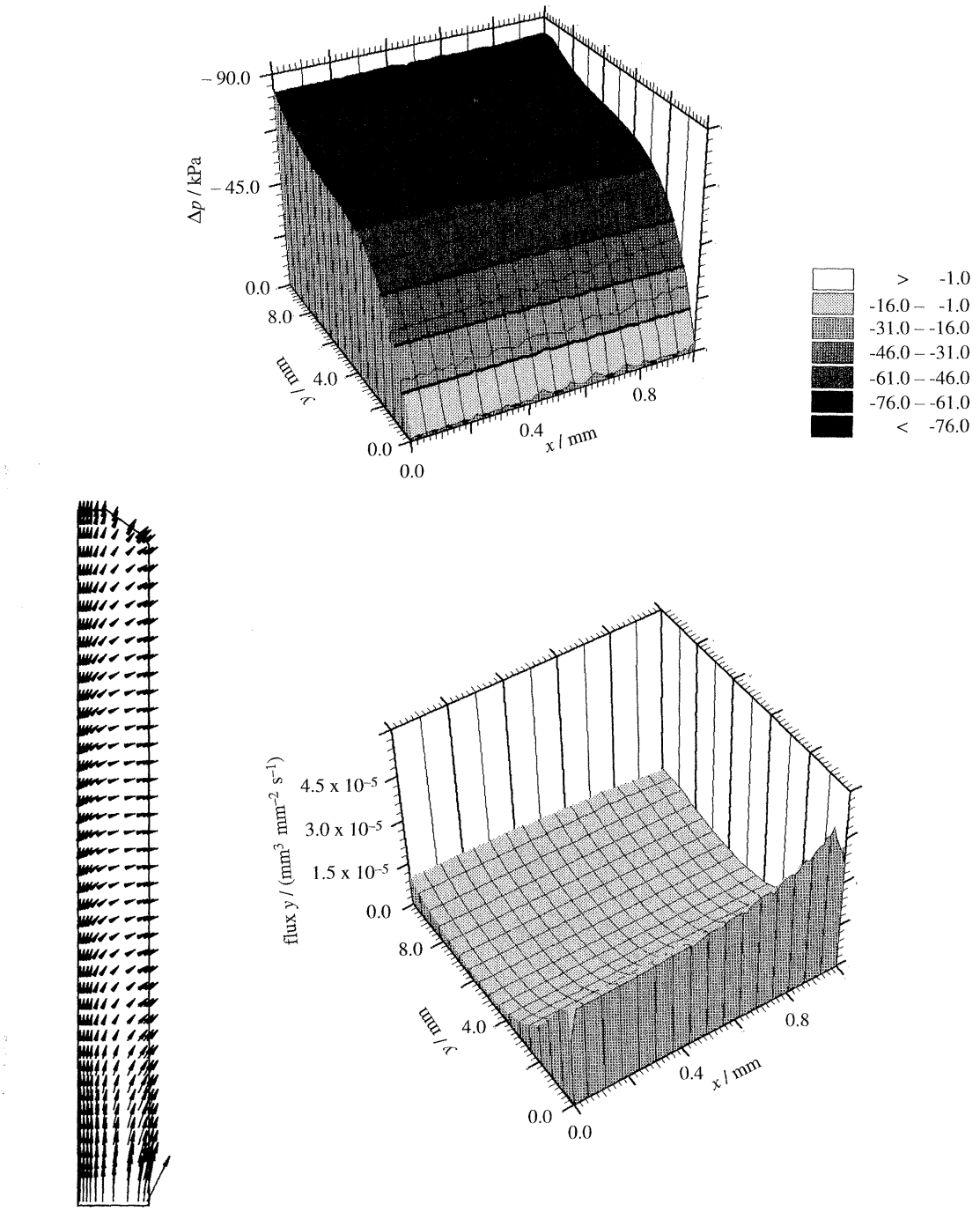

Figure 7. For description see figure 5.

v_y are small. Higher values occur only at the bottom and at the top. The pressure field changes during the following time steps. Finally, the fluid pressure gradient is parallel to the longitudinal axis leading to vertical fluxes: in steady state, which is attained after 7100 s, an acropetal transport stream is established with a fluid pressure of about −1000 kPa (= −1 MPa) near the top of the structure.

Figure 10 shows the pressure field of halfspace A3 in steady state which is attained at $T_{stat} = 600$ s. It is qualitatively identical to that of C3, but the values are less negative because of the reduced height of the axis. To allow for a direct comparison of different structures, the pressure values in steady state along the longitudinal axis at $X = 0.5$ mm of halfspaces A3, B3 and C3 are plotted against the Y-coordinates given as percent values of the total height of the entire grids (figure 11). Transpiration rate and hydraulic conductivity were varied for structure C3 (see table 1, structures C3b–C3d). The results regarding the temporal behaviour are listed in table 3 and illustrate that the hydraulic conductivity effects T_{stat} in a linear way. This effect is to be expected, because lower hydraulic conductivity means a correspondingly longer 'reaction time' of the system. This is due to the fact that at lower hydraulic conductivity the pressure gradient spreads more slowly. The transpiration rate, however, does not have any influence on

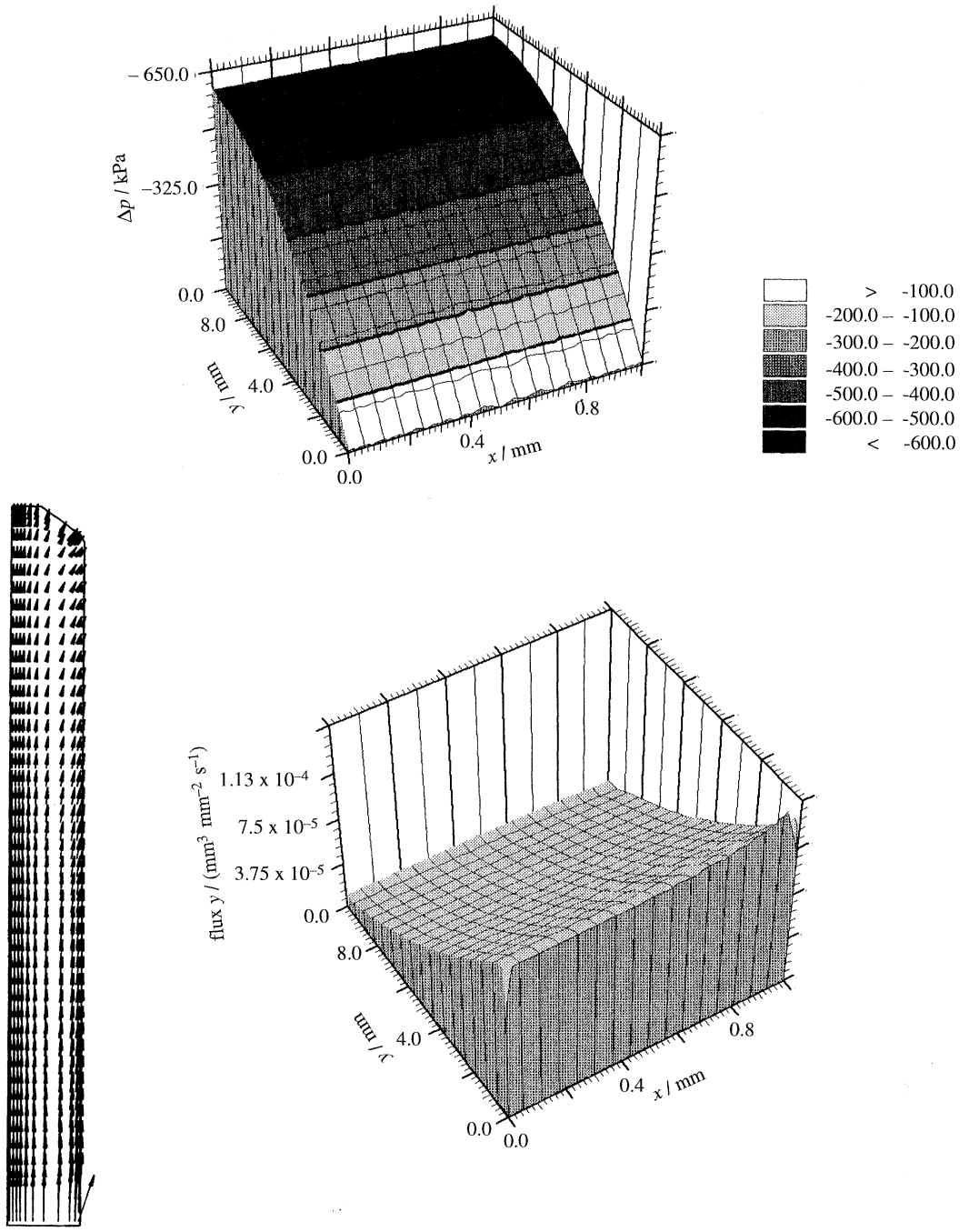

Figure 8. For description see figure 5.

T_{stat}. The equilibrium is therefore independent of the total water loss per time. Transpiration rate, hydraulic conductivity and pressure p show the expected linear relationships. This is demonstrated in figure 12.

The fluid pressure gradient in the model structure can also be reduced by broadening the axis. For instance, model structure B4, which is twice as thick as model structure C3 (cf. table 1), shows a fluid pressure gradient (figure 13) which is reduced by 50% as compared with C3 (figure 9). A simple explanation for this behaviour is that an increase of the radius entails a quadratic enlargement of the bottom or inflow area, but only a linear increase of the transpiring surface. This strategy of reducing the fluid pressure gradient in a parenchymatous plant by increasing the radius would finally lead to the development of a thallus.

At steady state, the system is in overall equilibrium. This implies that inflow equals outflow. Initially, however, the outflow exceeds the inflow until, at T_{stat}, both are in balance. The difference between in- and outflow causes a net loss of fluid. The temporal development of the inflow is represented in figure 14 for A3, B3 and C3; thereby inflow is expressed as percent values of the outflow at each time so that at T_{stat}, the inflow is 100% of the outflow. Obviously, the highest structure (C3) loses much more water than

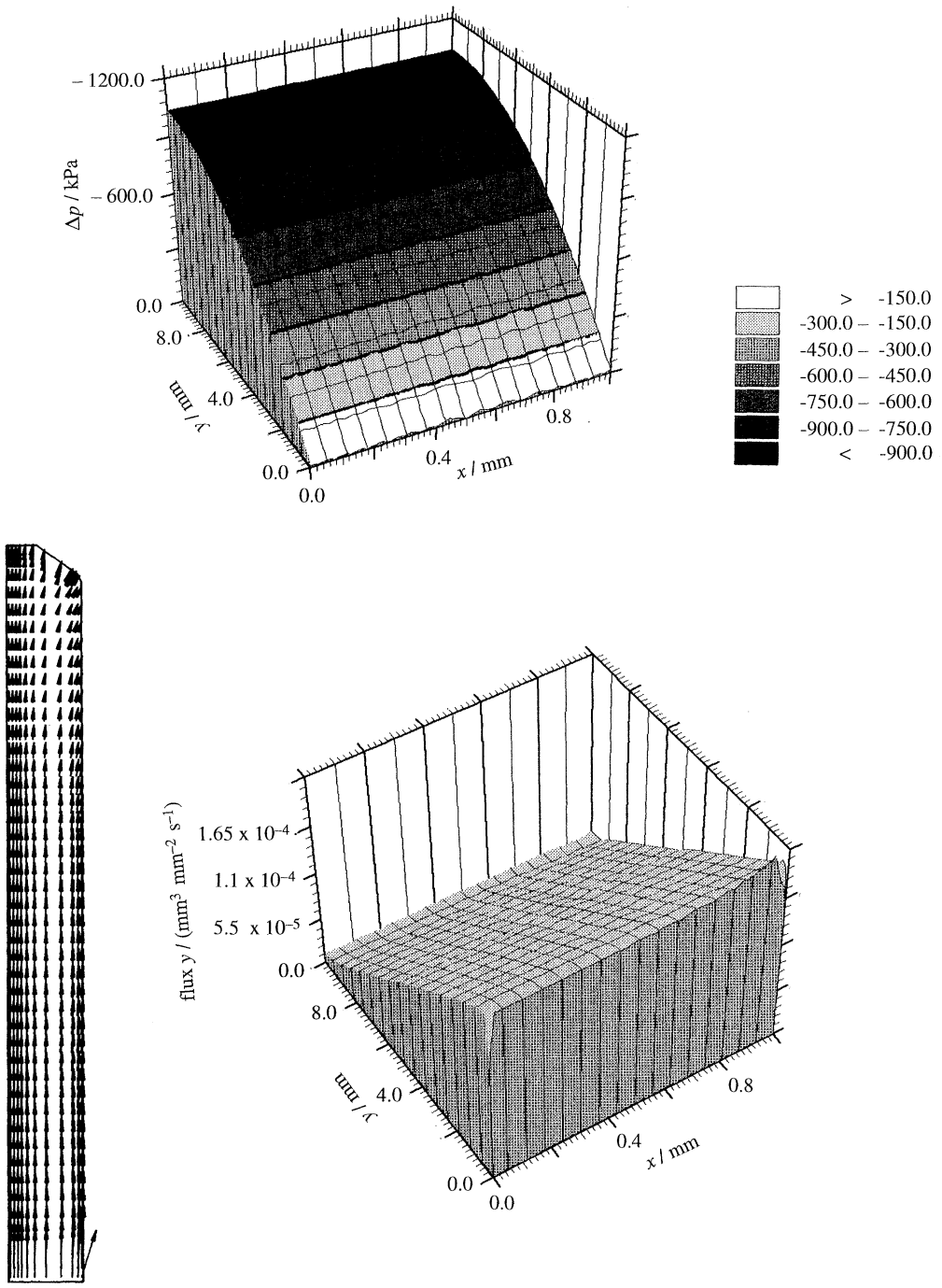

Figure 9. For description see figure 5.

the others (A3, B3). At $t = 1000$ s, only 70% of the fluid lost by structure C3 was recovered by inflow whereas A3 and B3 were already at steady state.

(*b*) *Homogeneous model with dynamic permeability*

Figure 15 and figure 16 show the distribution of hydraulic conductivities of models A (hydraulic conductivity is proportional to [negative] fluid pressure, figure 15) and B (hydraulic conductivity is inversely proportional to [negative] fluid pressure, figure 16; see above). Both systems are in steady state. In model A, the highest hydraulic conductivities developed directly at the transpiring surfaces; towards the inner regions of the axis hydraulic conductivities decrease. A narrow, peripheral layer of high hydraulic conductivity connects the surface directly with the basal fluid reservoir.

Model B shows the inverse pattern. Here, the highest hydraulic conductivities are located at the base of the structure and in the inner regions. The hydraulic conductivity decreases with height and distance from the centre of the axis. This model partly resembles a protostele but is more complex than a typical protostele. As in a protostele, the layer with the highest hydraulic conductivity is located at the centre of the axis, but the conductivity decreases also with height so that an inner cone-like structure results.

PHILOSOPHICAL TRANSACTIONS OF THE ROYAL SOCIETY B BIOLOGICAL SCIENCES

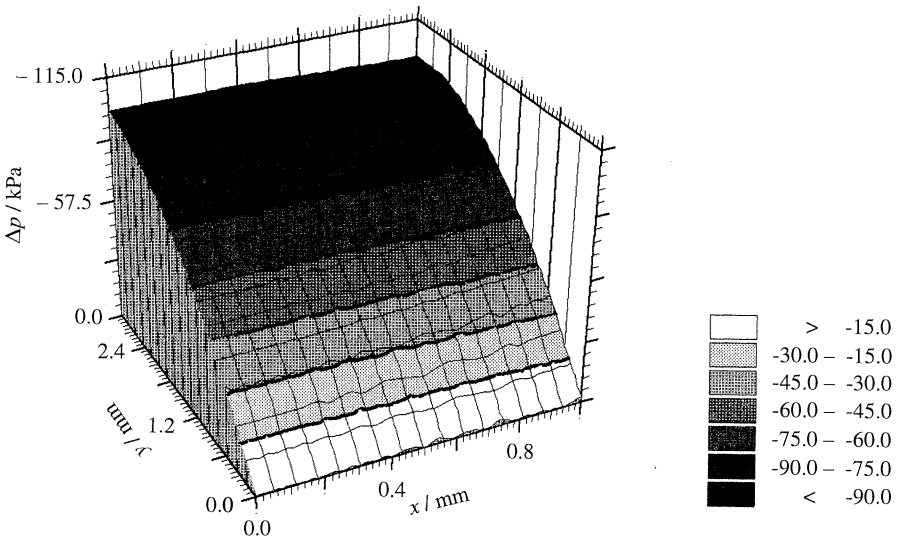

Figure 10. Structure A3 (radius = 1 mm, height = 3 mm, transpiration rate = 1×10^{-5} mm^3 mm^{-2} s^{-1}, hydraulic conductivity = 1×10^{-6} mm^2 s^{-1} kPa^{-1}): pressure field at $t = 600$ s = T_{stat}

7. DISCUSSION

The model calculations illustrate the limitations of parenchymatous water transport and the necessity for a more effective water transport system even in very small land plants. For a parenchymatous plant axis with a given hydraulic conductivity and transpiration rate, the height and radius of the structure determines hydrodynamic behaviour. In fact, the duration of the non-steady state and the magnitude of the fluid pressure gradient have to be regarded as characteristics of the transport efficiency because a rapid adaptation to changes of the transpiration rate and a smaller fluid pressure gradient reduce the stress on living tissue. The duration of the non-steady state increases exponentially with increasing height of the structure. For model structure C3 (radius = 1 mm, height = 10 mm, hydraulic conductivity = 1×10^{-6} mm^2 s^{-1} kPa^{-1}, transpiration rate = 1×10^{-5} mm^3 mm^{-2} s^{-1}) a time span of about 7000 s is required to reach steady state condition and a continuous net loss of water occurs during this time period. Thereby the value of the hydraulic conductivity used for structure C3 corresponds to the upper limit for parenchymatous tissue (Raven 1977) and a lower hydraulic conductivity would result in a corresponding prolongation of the non-steady state condition as was demonstrated by varying the hydraulic conductivity (cf. table 1).

However, the duration of the non-steady state does not depend on the transpiration rate. Correspondingly, if the plant is optimally supplied with water (as was simulated by the free boundary condition at the bottom), control of the transpiration rate by stomata does not influence the temporal behaviour of the system but only the absolute loss of water and the fluid pressure gradient: the higher the transpiration rate, the higher the water loss and the fluid pressure gradient will be.

At a given hydraulic conductivity and transpiration rate the fluid pressure gradient also depends on the

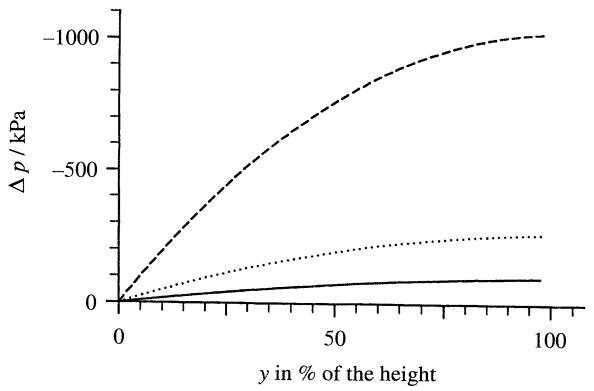

Figure 11. Pressure profiles at the steady state of structures A3 (solid line), B3 (dotted line) and C3 (dashed line) along the longitudinal axis at $X = 0.5$ mm. The Y-coordinates are given as percentage values of the total height of the structures in order to provide a direct comparison of the values (transpiration rate = 1×10^{-5} mm^3 mm^{-2} s^{-1}, hydraulic conductivity = 1×10^{-6} mm^2 s^{-1} kPa^{-1}). A3, 3 mm = 100%; B3, 5 mm = 100%; C3, 10 mm = 100%.

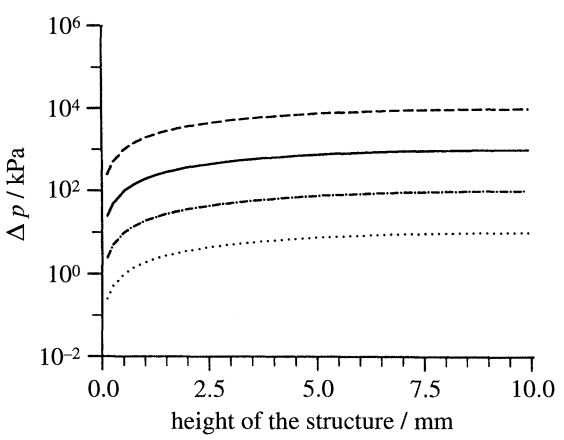

Figure 12. Pressure profiles along the longitudinal axis at $X = 0.5$ mm for the parametral variations of C3 (listed in table 1); C3, solid line; C3b, dotted line; C3c, dashed line; C3d, dot-dashed line.

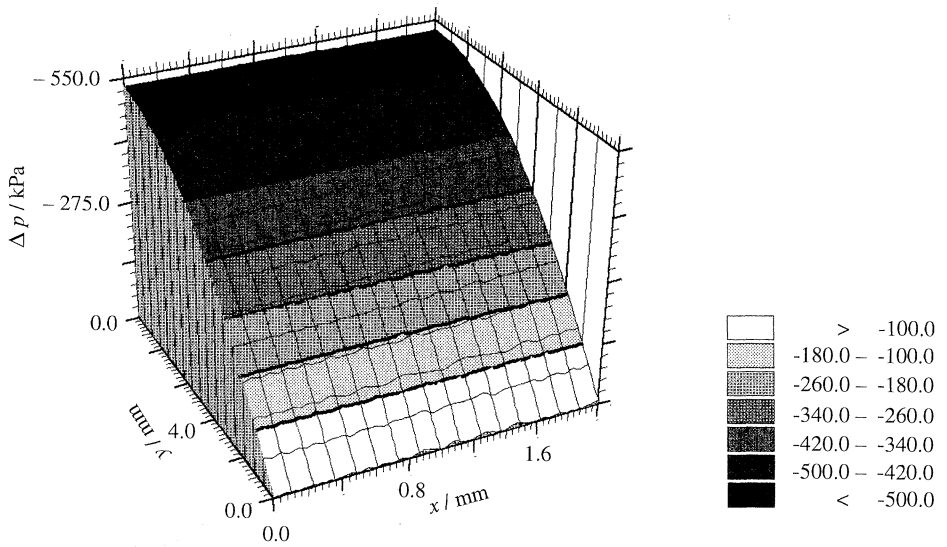

Figure 13. Pressure field of structure B4 (radius = 2 mm, height = 10 mm, transpiration rate = 1×10^{-5} $mm^3\,mm^{-2}\,s^{-1}$, hydraulic conductivity = 1×10^{-6} $mm^2\,s^{-1}\,kPa^{-1}$) at $t = T_{stat}$.

height of the axis. For halfspace C3 a gradient of about 1 MPa is developed at steady state condition. In more realistic cases, however, this gradient will be even higher because even moist soil has a negative water potential which has to be added to the fluid pressure gradient so that a transport stream from the soil to the transpiring surface can be established. Thus, when an unsaturated soil and a more realistic lower hydraulic conductivity of parenchyma is considered, a structure with a height of only 10 mm would develop a fluid pressure gradient well above 1 MPa.

Theoretically there exist three different ways to reduce the high fluid pressure gradient. One possibility is to enlarge the radius of the axis thus increasing the contact area between the water reservoir (soil) and the plant. This strategy would lead to a flat thalloid land plant as is observed, for instance, in some liverworts and land-living algae. Another possibility to reduce the fluid pressure gradient is to reduce the transpiration rate. Such a low transpiration rate is guaranteed in moist habitats and this is one of the reasons why many non-tracheophyte land plants are restricted to permanently humid environments. Anatomical structures such as a cuticle may also reduce the transpiration rate, but in this case the reduction in water loss is coupled with a reduction of the gaseous exchange. Hence, green land plants with a cuticle developed stomata for regulation of transpiration and gas exchange in order to achieve a compromise regarding water loss and the exchange of other gases.

A third possibility to reduce the fluid pressure gradient is to increase hydraulic conductivity in at least some parts of the plant axis and to establish a water transport system which is more effective than transport in parenchyma. In fact, our model results illustrate that a water conducting tissue is already essential for plants with a very small height. The upright posture has certain advantages for land plants because it exposes the photosynthesizing parts to sun light and improves dispersal of diaspores (Niklas *et al.* 1985). However, in a desiccating environment an erect and slender growth habit with a height of more than a few millimetres is only possible if a water conducting tissue exists because otherwise the fluid pressure gradient would become to large and the non-steady state would last too long. Similarily, in leaves the distance between vascular bundles is generally below 1 mm (Wylie 1939).

Thus the computer simulations of the water transport system in parenchymatous plant axes explain the early appearance of a water conducting system in land plants, because the demand for such a transport system became essential as the first erect land-dwelling plants evolved. This need for a water transport system in erect land plants of a certain height is further illustrated by many mosses which take up water from the soil and develop an internal conducting strand (if such a conducting strand is missing, then other water transport devices are used, such as capillary transport and water absorption by the surface, see below). The fluid velocities in these simple strands are comparable to those in woody

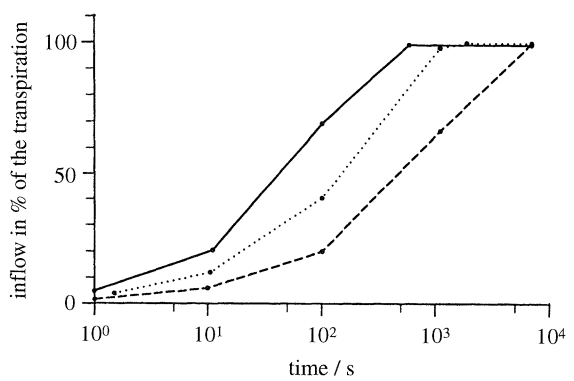

Figure 14. Temporal development of the inflow expressed as percentage value of the outflow, represented for structures A3 (solid line), B3 (dotted line) and C3 (dashed line). At T_{stat}, the inflow amounts 100% of the outflow.

PHILOSOPHICAL TRANSACTIONS OF THE ROYAL SOCIETY B BIOLOGICAL SCIENCES

15

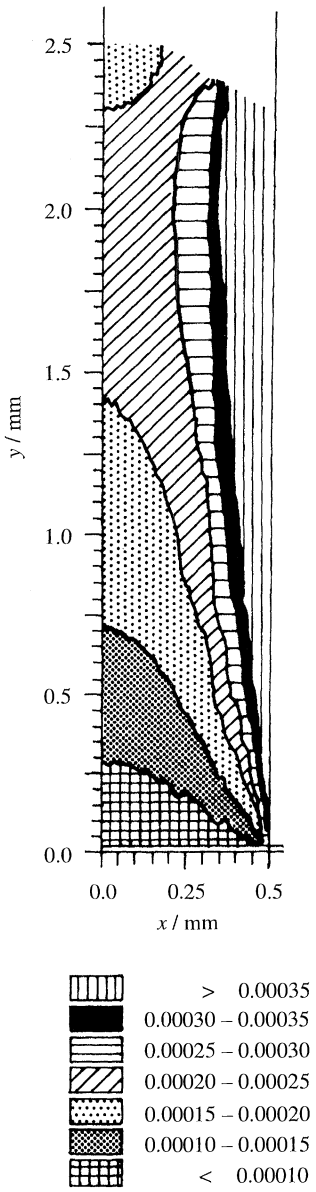

Figure 15. Increasing hydraulic conductivity with increasing negative fluid pressure.

16

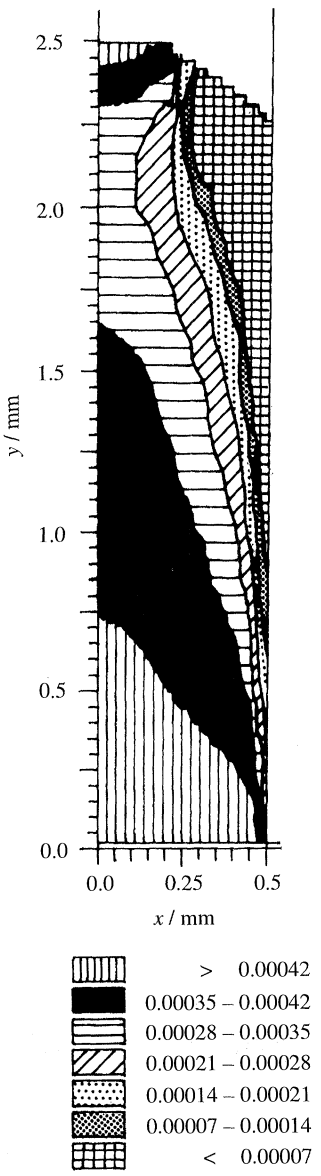

Figure 16. Decreasing hydraulic conductivity with increasing negative fluid pressure.

Figures 15 and 16. Patterns of hydraulic conductivity, represented as contour fields inside the corresponding half-space for the model structures with dynamic permeability. The functions describing the dependence of hydraulic conductivity on fluid pressure are shown in figure 3. The values of the hydraulic conductivity are given in the legends of the plots (dimension, $mm^2\,s^{-1}\,kPa^{-1}$).

plants (Zacherl 1954). In fact, the general mechanism of creating an effective water transport system is to increase the hydraulic conductivity of the apoplastic pathway by increasing its porosity. In nature, this is achieved in several ways. The conduits of vascular plants are provided by programmed cell death. In this case, a highly porous material is produced in which the lumina of the dead tracheary cells contribute to the void spaces. Mosses also use highly porous apoplastic pathways for water transport and these pathways are internal (as a central strand) or external. In the latter case a great variety of capillary devices are formed.

The model calculations with dynamic hydraulic conductivity describe the behaviour of structures with self-regulating hydraulic conductivities. In the case of increasing hydraulic conductivity with increasing negative pressure, layers with increased conductivity develop directly at the transpiring surface. This means, that water absorbed at the bottom is transported externally and can flow directly out of the structure due to transpiration. Such a conducting system is typical for plants with external water conduction, like, for example, the ectohydric mosses. Such organisms are usually restricted to moist habitats or are only physiologically active in moist surround-

PHILOSOPHICAL TRANSACTIONS OF THE ROYAL SOCIETY B BIOLOGICAL SCIENCES

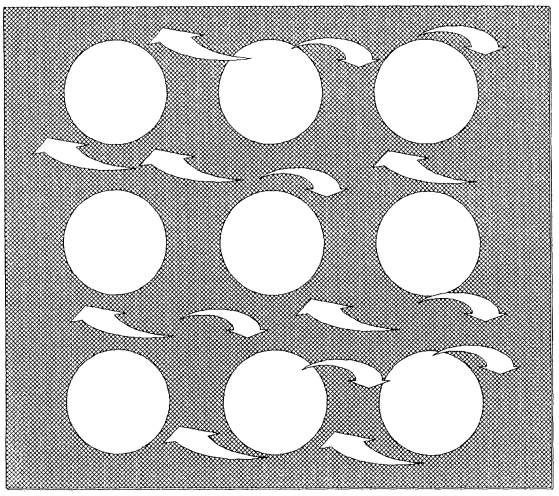

Figure 17. Schematic representation of the physical model system, which is composed of two phases, porous material matrix (hatched area) and fluid (white space).

ings. Another disadvantage of an external transport system is that it can not readily be used for distributing dissolved nutrients in the plants.

The inverse fluid pressure–permeability relationship, where hydraulic conductivity decreases with increasing negative fluid pressure, produces some kind of a central cone-like stele: the inner layers show the highest hydraulic conductivity which decreases with increasing distance from the bottom and the central axis. Along the free boundary at the bottom a layer with high hydraulic conductivity is developed thus providing an optimal utilization of the basal fluid reservoir.

The cone-like field with increased hydraulic conductivity resembles in a broad sense a protostele which has the form of a slightly tapering cylinder. The differences between a real protostele and the stele type resulting from the calculations are largely due to the mathematical model which allows for a linear and gradual increase of the local hydraulic conductivity. Hence, in the final stage of the mathematical model, there is a continuous variation from low hydraulic conductivity in the periphery to high hydraulic conductivity in the centre. In a real plant axis, however, a well-pronounced discontinuity exists between the hydraulic conductivity of parenchyma and xylem. Hence, in real plants, no continuous variation of hydraulic conductivity of the conducting elements exists.

Despite the limitations of our calculations with a continuous variation of hydraulic conductivity, model B clearly illustrates the tendency to form a protostele according to the corresponding pressure–permeability relationship. Therefore the protostele may be understood in terms of a self-regulating system in which hydraulic conductivity is a function of the fluid pressure and tends to be high in regions with a less negative water potential. This architecture is advantageous in several respects. The conducting strand is optimally isolated from the transpiring surface by parenchymatous tissue; the photosynthetic tissue can be located in the periphery and the water flow from the conducting strand through the parenchyma can be used to distribute dissolved nutrients.

As a whole, our modelling approach shows that the evolution of simple land plants was largely influenced by problems of water transport. The calculations demonstrate that there are several solutions to this problem which are all realized in nature. Land plants may try to reduce the distance of parenchymatous water transport by remaining flat and thalloid (e.g. liverworts). The evolution of a water transport system by development of a highly porous and therefore permeable apoplast provides another means to reduce the distance of parenchymatous water transport. This water transport system can be external (e.g. ectohydric mosses) or internal (e.g. endohydric mosses, tracheophytes). In general, an internal transport system proves to be more advantageous for several reasons (see above). Another – at least theoretical – strategy for solving the water transport problem would be to reduce the transpiration rate. A 'pure' version of this strategy is not realized in nature, because exchange of other gases would also be reduced. As a temporary strategy, however, it is found in tracheophytes during limited periods of drought leading to stomatal closure. All the modelling results are consistent with Nature and make it evident that the problems of water transport in plants can indeed be analysed theoretically by using a model system which describes the fluid flow in a poroelastic medium.

APPENDIX: THE MATHEMATICAL MODEL

A system consisting of two phases is considered; the two phases are a porous matrix and a fluid filling the void spaces (figure 17). The behaviour of the entire matrix-fluid structure is depending on the interactions occurring between these two components. The mathematical model describing the corresponding processes is based on the coupling of Darcy's law and Hooke's law. The fundamental approach is that of Biot (1941) who formulated a theory of porous rock compaction. Introducing the concept of dynamic permeability approach Grün *et al.* (1989) developed a system of nonlinear partial differential equations. It will be discussed briefly below (for a more detailed discussion of the theory of poroelastic media see, for example, Terzaghi (1923); Biot (1941); Crochet & Naghdi (1966); Grün *et al.* (1989); Wallner (1990)).

Certain assumptions for matrix and fluid are predicted: (i) the stress–strain relations are reversible; (ii) the elastic behaviour is linear; (iii) the fluid moves through the matrix according to the law of Darcy. The model contains the coupled equations of material matrix and fluid.

(*a*) *Material matrix*

The equation describing the mechanical behaviour of the material matrix is based on Hooke's law in its general form (the term 'material matrix' is used as synonymous to the porous medium):

$$\boldsymbol{\sigma}_{\text{eff}} = \mathbf{D}(\boldsymbol{\epsilon} - \boldsymbol{\epsilon}^{p}), \tag{1}$$

PHILOSOPHICAL TRANSACTIONS OF THE ROYAL SOCIETY B BIOLOGICAL SCIENCES

(in general, bold italic type denotes a vector and bold upright type denotes a matrix).

The effective stress $\boldsymbol{\sigma}_{\text{eff}}$ is depending on the strain $\boldsymbol{\epsilon}$ minus the hydrostatically caused strain $\boldsymbol{\epsilon}^{p}$ in a linear way. $\mathbf{D}$ represents the matrix of elasticity, which contains the material parameters Young's modulus and Poisson's ratio. $\boldsymbol{\epsilon}^{p}$ causes a dilatation which is due to the compressibility κ_{s} of the skeleton of the matrix. Because of the isotropic character of this process, the hydrostatic part of the extension can be described as ($\boldsymbol{m}$ = Dirac-Vector):

$$\boldsymbol{\epsilon}^{p} = -(\kappa_{s}/3)\, \boldsymbol{m}p. \tag{2}$$

As the structure is filled with fluid, which acts on the material, it has to be stated that elastic and hydrostatic (isotrop) components contribute to the total stress:

$$\boldsymbol{\sigma} = \mathbf{D}(\boldsymbol{\epsilon} - \boldsymbol{\epsilon}^{p}) - \boldsymbol{m}p. \tag{3}$$

Using equations (2) and (3) and by introducing the coupling coefficient $\boldsymbol{\beta}$ yields ($\boldsymbol{\beta} = \mathbf{I} - (\kappa_{s}/3)\mathbf{D}$, $\mathbf{I}$ = identity matrix):

$$\begin{aligned}\boldsymbol{\sigma} &= \mathbf{D}\boldsymbol{\epsilon} + (\mathbf{D}(\kappa_{s}/3)\, \boldsymbol{m}p) - \boldsymbol{m}p,\\ &= \mathbf{D}\boldsymbol{\epsilon} - (\mathbf{I} - (\kappa_{s}/3)\, \mathbf{D})\, \boldsymbol{m}p,\\ &= \mathbf{D}\boldsymbol{\epsilon} - \boldsymbol{\beta}\, \boldsymbol{m}p. \end{aligned} \tag{4}$$

The strain $\boldsymbol{\epsilon}$ can be expressed as displacement $\boldsymbol{u}$ of the material matrix coupled to the strain operator $\mathbf{L}$:

$$\boldsymbol{\epsilon} = \mathbf{L}\, \boldsymbol{u}. \tag{5}$$

According to the elastic behaviour of the matrix the equilibrium between forces is true:

$$\nabla^{\mathrm{T}} \boldsymbol{\sigma} + \boldsymbol{f}_{\mathrm{E}} = 0. \tag{6}$$

The extern forces are represented by $\boldsymbol{f}_{\mathrm{E}}$. Using equations (4), (5) and (6), the behaviour of the matrix can be described as follows (superscript $^{\mathrm{T}}$ denotes transpose of matrix):

$$\mathbf{L}^{\mathrm{T}}\, \mathbf{D}\mathbf{L}\, \boldsymbol{u} - \mathbf{L}^{\mathrm{T}}\, \boldsymbol{\beta}\, \boldsymbol{m}p + \boldsymbol{f}_{\mathrm{E}} = 0. \tag{7}$$

(*b*) *Fluid*

For the fluid flow the equation of continuity is true (Q = fluid accumulation, $\boldsymbol{v}$ = fluid velocity and q_{E} = flow rate per volume, superscript $'$ denotes time derivative):

$$\nabla^{\mathrm{T}} \boldsymbol{v} + q_{\mathrm{E}} = Q'. \tag{8}$$

The velocity of the flow, which is relative to the matrix, is determined by the gradient of the hydrostatic pressure, ∇p and the hydraulic conductivity, k. The latter quantity is expressed as tensor of permeability, $\mathbf{k}$.

$$\boldsymbol{v} = -\mathbf{k}\, \nabla p\, . \tag{9}$$

The permeability of a system may be a function of the effective pressure p_{eff}, that is the difference between pressure acting inside the material matrix and fluid pressure:

$$p_{\text{eff}} = -\sigma_{\mathrm{i}} - p\, , \tag{10}$$

with $\sigma_{\mathrm{i}} = 1/3\, \boldsymbol{m}^{\mathrm{T}}\, \boldsymbol{\sigma}_{\text{eff}}$.

In this case, the system of differential equations is nonlinear. The fluid accumulation Q depends on several processes, such as matrical deformations provided by external forces and volumetric changes due to hydrostatic pressure. These different factors can be summarized as follows (κ = compressibility of the entire system):

$$Q' = \boldsymbol{m}^{\mathrm{T}}\, \boldsymbol{\beta}\, \boldsymbol{\epsilon}' + \kappa p'. \tag{11}$$

This means that Q is proportional to the time derivatives of the deformation and the fluid pressure. As described above, the hydraulic permeability can be a function of the effective pressure, which is the difference between pressure inside the matrix and fluid pressure. The system of differential equations will be nonlinear in this case. At least, using equations (8), (9) and (10), the following term describing the behaviour of the fluid phase is obtained:

$$-\nabla^{\mathrm{T}}(\mathbf{k}\, (p_{\text{eff}})\, \nabla p) + q_{\mathrm{E}} = \boldsymbol{m}^{\mathrm{T}}\, \boldsymbol{\beta}\, \mathbf{L}\boldsymbol{u}' + \kappa p' \tag{12}$$

Equations (7) and (12) represent a system of coupled differential equations describing the behaviour of the entire structure composed of matrix and fluid.

This work was supported by the Deutsche Forschungsgemeinschaft (SFB 230) and by a grant from the University of Bonn (Graduiertenförderungsgesetz Nordrhein-Westfalen) to A.R.

REFERENCES

Altman, P.L. & Dittmer, D.S. (eds) 1973 *Biology data book.* 2nd edn, vol. II. Bethesda: Federation of American Societies for Experimental Biology.

Bear, J. 1972 *Dynamics of fluids in porous media.* New York: Elsevier.

Bear, J. 1979 *Hydraulics of groundwater.* New York: Elsevier.

Biot, M.A. 1941 General theory of three-dimensional consolidation. *J. appl. Phys.* **12**, 155–164.

Boyer, J.S. 1985 Water transport. *A. Rev. Pl. Physiol.* **36**, 473–516.

Bower, F.O. 1908 *The origin of land flora.* London: Macmillan.

Burström, H.G., Uhrström, I. & Olausson, B. 1970 Influence of auxin on Young's modulus in stems and roots of *Pisum* and the theory of changing the modulus in tissues. *Physiol. Pl.* **23**, 1223–1233.

Canny, M.J. 1989 What becomes of the transpiration stream? *New Phytol.* **114**(3), 341–368.

Carlquist, S. 1975 *Ecological strategies of xylem evolution.* Berkeley, Los Angeles, London: University of California Press.

Chappell, T.W. & Hamann, D.D. 1968 Poisson's ratio and Young's modulus for apple flesh under compressive loading. *Trans. Am. Soc. agric. Engin.* **11**, 608–610.

Crochet, M.J. & Naghdi, P.M. 1966 On constitutive equations for flow of fluid through an elastic solid. *Int. J. Engin. Sci.* **4**, 383–401.

Edwards, D., Davies, K.L. & Axe, L. 1992 A vascular conducting strand in the early land plant *Cooksonia*. *Nature, Lond.* **357**, 683–685.

Edwards, D. & Fanning, U. 1985 The microfossil record of early land plants: advances in understanding of early terrestrialization. *Phil. Trans. R. Soc. Lond.* B **309**, 147–166.

PHILOSOPHICAL TRANSACTIONS OF THE ROYAL SOCIETY B BIOLOGICAL SCIENCES

Falk, S., Hertz, C.H. & Virgin, H.I. 1958 On the relation between turgor pressure and tissue rigidity. *Physiol. Pl.* **11**, 802–817.

Gray, J. 1985 The microfossil record of early land plants: advances in understanding of early terrestrialization. *Phil. Trans. R. Soc. Lond.* B **309**, 167–195.

Grün, G.-U., Wallner & H., Neugebauer, H.J. 1989 Porous rock deformation and fluid flow—numerical FE-simulation of the coupled system. *Geologische Rundschau* **78**(1), 171–182.

Koehl, M. & Wainwright, S.A. 1977 Mechanical adaptations of a giant kelp. *Limnol. Oceanogr.* **22**, 1067–1071.

Marsily, G., de 1986 *Quantitative hydrogeology*. London, New York: Academic Press.

Molz, F.J. 1976 Water transport through plant tissue: the apoplasm and symplasm pathways. *J. theor. Biol.* **59**, 277–292.

Molz, F.J. & Ferrier, J.M. 1982 Mathematical treatment of water movement in plant cells and tissue: a review. *Pl. Cell Environ.* **5**, 191–206.

Mosbrugger, V. 1990 The tree habit in land plants. (*Lect. Notes Earth Sci.* **28**.) Heidelberg, Berlin, New York: Springer Verlag.

Niklas, K.J. 1988 Dependency of the tensile modulus on transverse dimensions, water potential, and cell number of pith parenchyma. *Am. J. Bot.* **75**(9), 1286–1292.

Niklas, K.J. & Kerchner, V. 1984 Mechanical and photosynthetic constraints on the evolution of plant shape. *Paleobiology* **10**, 79–101.

Niklas, K.J., Tiffney, B.H. & Knoll, A.H. 1985 Patterns in vascular land plant diversification: an analysis at the species level. In: *Phanerozoic diversity patterns – profiles in macroevolution* (ed. J. W. Valentine), pp. 97–128. Princeton University Press.

Nobel, P.S. 1983 *Biophysical plant physiology and ecology*. San Francisco: W. H. Freeman and Co.

Proctor, M.C.F. 1982 Physiological ecology: water relations, light and temperature responses, carbon balance. In *Bryophyte ecology* (ed. A. J. E. Smith), pp. 333–381. London: Chapman and Hall.

Raven, J.A. 1977 The evolution of vascular land plants in relation to supracellular transport processes. *Adv. Bot. Res.* **5**, 153–219.

Raven, J.A. 1984 Physiological correlates of the morphology of early vascular plants. *Bot. J. Linn. Soc.* **88**, 105–216.

Schulte, P.J. 1992 The units of currency for plant water status. *Pl. Cell Environ.* **15**, 7–10.

Slatyer, R.O. 1967 *Plant-water relationships*. London, New York: Academic Press.

Speck, T. & Vogellehner, D. 1988 Biophysical examinations of the bending stability of various stele types and the upright axes of early 'vascular' plants. *Bot. Act.* **101**, 262–268.

Stebbins, G.C. & Hill, G.J.C. 1980 Did multicellular plants invade the land? *Am. Nat.* **115**(3), 342–353.

Terzaghi, K. 1923 Die Berechnung der Durchlässigkeitsziffer des Tones aus dem Verlauf der hydrodynamischen Spannungserscheinung. *Sitzungsber. Akad. Wiss. Wien Math.-Naturwiss. Kl. Abt. IIA* **132**, 125–138.

Vincent, J.F.V. 1990 Fracture properties of plant materials and structures. *Adv. Bot. Res.* **17**, 252–287.

Wallner, H. 1990 Finite Elemente Simulation von Fluidbewegungen in einem deformierbaren poroelastischen Medium mit druckabhängiger Permeabilität. Ph.D. thesis, TH Clausthal.

Weast, R.C. & Astle, M.J. (eds) 1983 *CRC handbook of chemistry and physics*. Boca Raton, Florida: CRC Press.

Westgate, M.E. & Steudle, E. 1985 Water transport in the midrib tissue of maize leaves. *Pl. Physiol.* **78**, 183–191.

Wylie, R.B. 1939 Relations between tissue organization and vein distribution in dicotyledon leaves. *Am. J. Bot.* **26**, 219–225.

Zacherl, H. 1954 Physiologische und ökologische Untersuchungen über die innere Wasserleitung bei Laubmoosen. Ph.D. thesis, Universität München.

Zienkiewicz, O.L. & Taylor, R.L. 1989 *The finite element method*, 4th edn, vol. 1. London, New York: McGraw-Hill.

Zimmermann, W. 1959 *Die Phylogenie der Pflanzen*. Stuttgart: Gustav Fischer Verlag.

Zimmermann, W. 1952 Main results of the 'Telome Theory'. *Paleobotanist*, Birbal Sahni Memorial Volume, 456–470.

Received 18 October 1993; accepted 19 January 1994

PHILOSOPHICAL TRANSACTIONS OF THE ROYAL SOCIETY B BIOLOGICAL SCIENCES